

The Hadron Spectrum from Lattice QCD*

C. B. Lang

Inst. f. Physik, FB Theoretische Physik,
Universität Graz, A-8010 Graz, Austria

November 6, 2018

Abstract

Determining the hadron spectrum and hadron properties beyond the ground states is a challenge in lattice QCD. Most of these results have been in the quenched approximation but now we are entering the dynamical era. I review some of the ideas and methods of the lattice approach, concentrating on a few examples and on results obtained for Chirally Improved (CI) fermions.

1 Introduction

1.1 Motivation

This lecture reviews some methods to compute the masses of hadrons in lattice QCD. The emphasis lies on the low lying excited states. In the spirit of the school I try to combine an introduction to the field with a presentation of some recent work. Most of the results for masses presented here are based on work within the Bern-Graz-Regensburg (BGR) collaboration. As a motivation let me start with some results obtained for the so-called quenched situation, where the fermion loops of the vacuum are disregarded.

In that approximation the quarks are valence quarks and it is comparatively simple to work at several quark masses. Since one cannot (yet) compute at small enough quark masses, one extrapolates the values obtained from higher masses (corresponding to pion masses around and above 300 MeV) down to the fictitious chiral limit, where the current quark masses of the up and the down quarks vanish. Since this is close to the physical case, it provides a useful standard for comparison of different computations. Fig. 1 gives the results for the low lying baryons (in the situation $m_u = m_d = 0$ and m_s such that the kaon mass has its experimental value).

There are some observations to be made:

- Ground state and first excitations are clearly seen. The negative parity states are close to their experimental values. Four states (positive parity: Ω excitation near 2.3 GeV, negative parity: two Ξ states near 1.78 GeV and a Ω ground state near 1.97 MeV) are seen, which are not established in the Particle Data Group tables. Both negative parity states $N(1535)$ and $N(1650)$ are seen.

*Notes based on a lecture at the Int. School of Nuclear Physics, 29th Course, 16-24. Sept. 2007, Erice/Sicily, "Quarks in Hadrons and Nuclei"

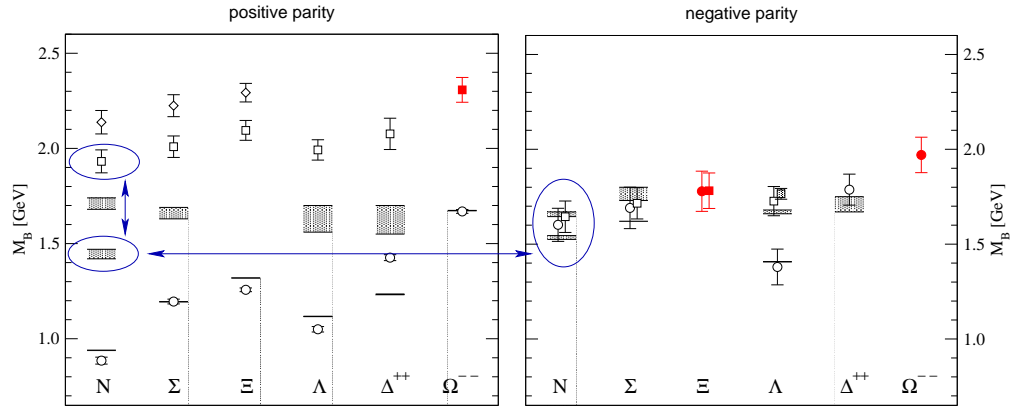


Figure 1: The chiral extrapolations of the positive parity (left) and negative parity (right) low lying baryons [1].

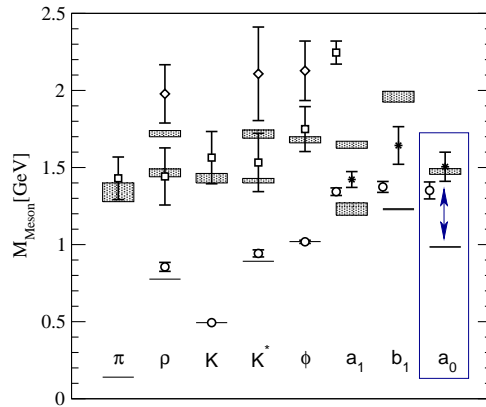


Figure 2: The chiral extrapolations of the low lying mesons [2].

- The excitations in the positive parity sector are clearly too high. In particular the Roper state $N(1440)$ comes out 30% too heavy. Since the standard level ordering is seen for the heavy quark region, one expects a level crossing of the $N(1535)$ and the Roper towards physical quark masses. This is not observed in these calculations.

The usual suspects are finite volume effects and the missing dynamical fermions.

Fig. 2 gives the meson results for that quenched study [2]. Here we find that the ground state of the isovector scalar meson a_0 (emphasized by the surrounding box in the figure) is either not seen or comes much too high, i.e., where the first excitation $a_0(1450)$ is measured. Again it would be important to find out how fully dynamical sea-quarks would affect this picture.

Let us summarize the challenges and questions:

- What effects have dynamical quarks on the excitations, in particular towards smaller, physical quark masses?
- What is the role of chiral symmetry (and its breaking)? Is there a “symmetry restoration” [3] towards higher excitations?
- How can we improve the analysis method and get even higher excitations? How to get properties like coupling constants and decay constants for the excited states?

1.2 Lattice QCD

Let me start with a “Declaration of QCD”: We assume that QCD is *the* quantum field theory of quarks and gluons, defined by a Lagrangian and action of the form

$$L = \frac{1}{2g^2} \text{tr} F_{\mu\nu} F_{\mu\nu} + \sum_f \bar{\psi}_f (\not{D} + m_f) \psi_f, \quad (1)$$

$$S = \int d^4x L.$$

We have formulated the theory in Euclidean space-time for convenience. The sum is over the quark flavors, \not{D} denotes the usual Dirac operator. We furthermore assume that this theory can be solved from first principles, with a minimal number of experimental input parameters (the bare quark masses and a scale fixing parameter) and that all hadron properties should be computable that way.

Quantization of such a field theory may be done with a path (functional) integration. A two-point function describing the propagation of a nucleon would be evaluated through

$$C_N(t) = \langle \bar{N}_t N_0 \rangle \propto \int [\mathcal{D}A \mathcal{D}\bar{\psi} \mathcal{D}\psi] e^{-S(A, \bar{\psi}, \psi)} \bar{N}_t N_0 \sim \exp(-E_N t). \quad (2)$$

Assuming that the nucleon is at rest, the asymptotic exponential behavior is determined by its mass. In Fig. 3 such a propagation of a meson is shown schematically. In the path integral fermions are represented by Grassmann-variables and can be integrated explicitly. The result is the determinant of the Dirac operator, which acts as a weight in the path integral over the gauge fields. Neglecting the determinant amounts to neglecting the vacuum quark loops, the so-called quenched approximation.

Ken Wilson suggested more than 30 years ago [4] to formulate QCD on a Euclidean space time lattice. This way the functional integral is high-dimensional but well defined. The quark fields ψ become Grassmann variables defined on the lattice sites and the color gauge fields are represented by SU(3)-matrices $U_\mu(x)$ living on the links connecting the sites. The Dirac operator becomes just a (very, very large) matrix. This formulation opened the way to non-perturbative path integration with the help of computers. Obviously it is an approximation and one has to study whether the approximation makes sense and leads to stable results in the continuum limit, as discussed below. Lattice QCD provides a gauge invariant definition of QCD as a quantum field theory. As formulated it is an approximation, which may be improved by various techniques, but it is QCD and not a model of QCD-phenomenology.

A few years after Wilson’s suggestion actual calculations were done for Yang-Mills theory, starting with Mike Creutz’ seminal suggestion [5] how to use Monte Carlo methods to compute the path integral

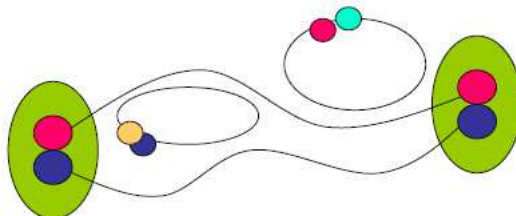


Figure 3: Schematic propagation of a meson. The closed quark-loops are neglected in the so-called quenched approximation.

for the gauge fields. Meanwhile lattice field theorists have entered prominently the crowd of high demand and high performance computer users. Quenched calculations have become well controlled. There the gluon interactions are covered completely non-perturbatively. Valence quarks on the gluonic background are done in various contexts and many of the results have been – given the quenched approximation – in surprising agreement with experiments. The issue nowadays is to include fermions fully dynamically, i.e., including the fermion determinant in the path integral weight.

In QCD there are $n_f + 1$ parameters, corresponding to the scale and the n_f current quark masses. In the lattice formulation these are dimensionless parameters like the gauge coupling and the bare quark masses. The calculation produces n-point functions, and the first results have been for propagators of QCD bound states like the pion or the nucleon. The exponential decay (2) gives the dimensionless exponent $Mt = (aM)(t/a)$, where a denotes the lattice spacing in physical units.

We thus get dimensionless masses aM from this analysis and have to set the scale a . The lattice spacing changes with the bare parameters of the simulations and these have to be tuned in order to approach the continuum limit phase boundary, which is where $a(g, m) \rightarrow 0$ (m symbolizes the set of all bare quark masses). Optimally one would follow trajectories in the parameter space where mass ratios are fixed to their physical values. Due to the enormous computational cost this is not always possible and one relies on patchwork combining results for different domains of the parameters.

Given the physical mass M and from the measurement the dimensionless lattice mass aM , one can determine the lattice spacing for the simulation set of parameters. Using $n_f + 1$ physical numbers (like, e.g., bound state masses or decay constants) one can, in principle, fix all unknown quantities and therefrom compute all physics contained: other masses, decay constants, matrix elements, scattering amplitudes and so on.

Practical calculations are restricted to finite sets of numbers and finite computer resources. In that sense the lattice simulations are approximations. We are interested in understanding three limits in our calculations.

Continuum limit $a(g, m) \rightarrow 0$: This is obtained for the bare gauge coupling $g \rightarrow 0$ and the mass parameters adjusted such that mass ratios remain constant. Different lattice actions correspond to different quality of approximations. In a perturbative expansion the Wilson gauge action has corrections $\mathcal{O}(a^2)$ and the Wilson fermion actions $\mathcal{O}(a)$. There are various attempts to improve that behavior, mostly based on either perturbative concepts (the Symanzik improvement program) or non-perturbative concepts (like real space renormalization transformations). There are now improved fermion actions which have corrections of only $\mathcal{O}(a^2)$. One hopes to obtain results closer to the continuum situation if these corrections are small. Typical lattice spacing values in full QCD simulations lie between 0.07 and 0.2 fm.

Thermodynamical limit $L \rightarrow \infty$: Assuming the lattice has L^4 sites, its physical extension is aL . Ideally one wants to keep that physical size reasonable large (several fm) and constant when $a \rightarrow 0$. Therefore L has to grow correspondingly when reducing the lattice spacing (cf. Fig. 4).

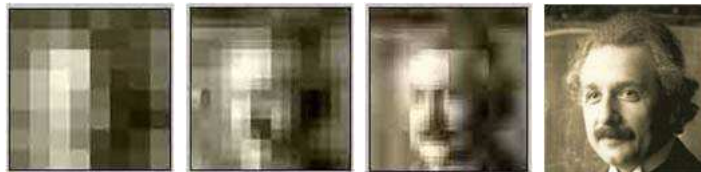


Figure 4: The same physical image represented on lattices of linear extent 8, 16, 32, and 128 corresponding to lattice spacings of 4 cm, 2 cm, 1cm, and 1/4 cm.

Chiral limit $m \rightarrow 0$ or physical quark mass limit $m \rightarrow m_0$: It is substantially harder to simulate at smaller quark masses. This is related to numerical problems like matrix inversion and to the effect of increasing correlation lengths (smaller pion mass). For that reason one has so far worked at relatively large bare quark masses corresponding to pion masses around 400 MeV and higher. On the other hand, real life occurs at small quark masses and a pion of 140 MeV. This is close to the chiral limit where quarks and pions are massless due to spontaneous chiral symmetry breaking.

In that limit we have some understanding of the effective theory, notably chiral perturbation theory (ChPT) [6]. This helps to analyze the approach from higher towards smaller quark masses. Present day results indicate that one has to have pion masses below 300 MeV to clearly identify terms of the effective theory.

2 Fermions and chiral symmetry

2.1 *The Ginsparg-Wilson condition*

In continuum the massless Dirac operator anti-commutes with γ_5 ,

$$\not{D}\gamma_5 + \gamma_5 \not{D} = 0 . \quad (3)$$

This leads to a decoupling of left-handed and right-handed modes. If the light quarks are massless, the chiral symmetry $SU(2)_L \times SU(2)_R$ is broken spontaneously by the strong interaction and there is a massless Goldstone triplet, the pion. In reality the light quarks have small, but non-vanishing masses leading to an additional explicit breaking of the symmetry giving rise to the light pions. This behavior may be described by ChPT.

In order to show that there is spontaneous symmetry breaking, a theory should allow for chiral symmetry for vanishing quark masses. Otherwise we cannot be sure, that the mechanism is as expected. Unfortunately the lattice formulation does not allow for a chirally symmetric formulation like in the continuum. There is a fundamental theorem [7] stating that under quite general conditions chiral symmetry on the lattice cannot be realized without invoking additional fermions (so-called doublers). The original formulation of Wilson pairs left-handed and right-handed fermions.

In a seminal paper Ginsparg and Wilson [8] suggested a condition which formulates chiral symmetry on the lattice in a modified form. Based on renormalization group arguments they proposed to replace (3) by another equation, which in a simple version may be written

$$D \gamma_5 + \gamma_5 D = a D \gamma_5 D . \quad (4)$$

The right-hand side vanishes in the continuum limit and full continuum chiral symmetry is recovered. This suggestion was considered infeasible in practice and the paper was essentially ignored until the late 1990ies, when it was realized that there are indeed possible realizations [9, 10] of that concept. Eventually a lattice version of the chiral rotations was formulated [11] which leaves the massless lattice action, if obeying the Ginsparg-Wilson condition (GWC), invariant.

2.2 *Fermion species*

What fermions are on the market and what are their advantages or disadvantages? There are two main groups: GW-type and non-GW-type. In the first group the most prominent representatives are

- Wilson improved: The original Wilson fermion action which does have doubler modes with masses $\mathcal{O}(1/a)$, improved by an extra term which has the correct dimension to correct for chiral symmetry. Its coefficient has to be adjusted non-perturbatively which corrects the additively renormalized

fermion mass. One of the technical problems is the occurrence of spurious zero modes of the Dirac operator for smaller (but non-zero) quark masses. The spurious modes turn up randomly for the sampled gauge configurations. This prevents computations at small quark masses unless one goes to very large lattices and small lattice spacing, where the situation improves.

- Staggered fermions: The fermionic degrees of freedom are distributed over hypercubes and a remnant chiral symmetry is sustained. Since there is no additive fermion mass renormalization, this formulation is convenient to simulate. There are, however, still too many fermions (a factor of 4 instead of 16 for the Wilson fermions) and these “tastes of fermions” confuse the identification of the hadron states. It is presently disputed, whether the theory has a correct continuum limit.
- Twisted mass fermions: An extra term in the Wilson action changes the eigenvalue spectrum of the Dirac operator such that there are no spurious modes. The theory breaks parity and flavor symmetry; this is recovered in the continuum limit, though.

The most prominent representative in the group of GW-type actions is the **overlap Dirac operator** [10]. The massless operator is an explicit construction,

$$D_{\text{ov}} = \frac{1}{a} [1 + \gamma_5 \text{sign}(\gamma_5 A)] , \quad (5)$$

where A is a kernel operator like, e.g., the usual Wilson operator, evaluated at negative quark masses. The technical problem is to compute the sign function of the huge matrix $(\gamma_5 A)$. So far this operator has been used mainly for quenched calculations, i.e., for the valence quark propagators. It is technically very demanding to implement it for dynamical fermions and attempts in this direction are under progress by various groups. With the massless overlap operator one may have single left- or right handed zero modes.

The **domain wall action** [12, 13] uses an extra 5th dimension in order to separate left-handed from right-handed modes and approaches the overlap operator in the limit of infinite extension in the 5th direction.

A perfect operator would be one that lies on a renormalized trajectory. An approximation to that is the **fixed point operator** [9], which lies close to such a trajectory and also has good, but not perfect, chiral properties.

Another approximate GW-type operator is the so-called **chirally improved operator** (CI-fermions) [14], which has been constructed from a systematic expansion in terms of nearest-neighbor, next-to-nearest-neighbor etc. terms, plugged into the GWC and solved algebraically. Since the expansion has to be truncated, the GWC is obeyed only approximately, like in the case of the fixed point or the domain wall action.

In the BGR collaboration we have been studying both, the fixed point and the CI operators [15]. Both show good chiral behavior and allow to approach smaller pion masses than is possible with the improved Wilson action for same size lattices. The actions have many more terms and are an order of magnitude more expensive to simulate than the simpler non-GW-type actions. However, they are still about an order of magnitude cheaper than expected for the overlap action. For the rest of this presentation I will restrict myself to showing results from my collaboration based on CI fermions.

3 Excited states

3.1 How to obtain particle masses

Masses are measured through real space propagators of the form

$$C_X(\vec{p}, t) = \langle X(\vec{p}, t) \bar{X}(\vec{p}, 0) \rangle \quad \text{with} \quad X(\vec{p}, t) = \sum_{\vec{x}} \hat{X}(\vec{x}, t) e^{-i\vec{x}\cdot\vec{p}} . \quad (6)$$

The hadron interpolators X are chosen with specified Lorentz-, Dirac-, flavor-, and color symmetries. We have projected the real space operators to a fixed 3-momentum \vec{p} . The propagation functions will vanish if conservation laws due to these symmetries are violated, e.g., if one combines an operator with the quantum numbers of a pion as source with that of a rho-meson as a sink. Simple meson field operator will have a form like $\bar{d}(x)\gamma_5 u(x)$ for the π^+ but can be more complicated involving also non-local but gauge invariant terms like $\bar{d}(x)\gamma_5 U(x,y)u(y)$ where U denotes a product of gauge field link variables connecting x with y .

When integrating over the Grassmann variables, the correlation function is expressed in terms of matrix elements of the inverted Dirac operator, i.e., the quark propagator. Eq. (2) becomes an integral over the gauge field variables with $\det(D + m_f)$ as weight factor and products of quark propagator matrix elements $(D + m_f)_{xy}^{-1}$ in the integrand,

$$C_\pi(x \rightarrow y) \propto \int [\mathcal{D}U] e^{-S_{\text{gauge}}(U)} \left(\prod_f \det(D + m_f) \right) \text{tr} \left((D + m_u)_{xy}^{-1} \gamma_5 (D + m_d)_{yx}^{-1} \gamma_5 \right) . \quad (7)$$

The integration thus reduces to finding gauge configurations sampled according to the weight from the gauge action and the fermion determinant(s). On each such gauge configuration one computes the quark propagators from some source point to all other points of the lattice by inverting the Dirac operator matrix $(D+m)$. Combination of the quark propagators gives the contribution to the correlation functions. This is repeated for as many gauge configurations as possible.

Projecting to $\vec{p} = 0$ simplifies the analysis, since the energy of the hadron at rest is just its mass. Due to the usually chosen boundary conditions a meson propagator is periodic and will have contributions from propagation forward as well as backward in Euclidean time,

$$C_\pi(\vec{p} = 0, t) \sim e^{-am_\pi t} + e^{-am_\pi(T-t)} , \quad (8)$$

where t denotes the time in lattice units and T is the extent of the lattice in temporal direction. The above behavior is only asymptotically, for large temporal distances. For smaller values of t higher excitations will modify the functional form. This is one of the issues to be discussed later. Computing the pion mass leads to results like the GMOR relation $m_\pi^2 \propto m_q$, which has been verified in many lattice calculations (see, e.g., [15]).

The construction of the interpolating field operators is inspired by the heavy quark limit. Remember, that site fields correspond to fields implicitly averaged over lattice distances of a . Almost any operator with the correct quantum numbers should do, although bad choices may not couple strongly to the physical state. The correlation function will have a larger amplitude if the overlap with the physical state is better and thus the signal improves.

There is some freedom for choosing the hadron interpolating fields. Simple examples like the nucleon-type operator

$$N^{(i)} = \epsilon_{abc} \Gamma_1^{(i)} u_a \left(u_b^T \Gamma_2^{(i)} d_c - d_b^T \Gamma_2^{(i)} u_c \right) . \quad (9)$$

with the choices

	$\Gamma_1^{(i)}$	$\Gamma_2^{(i)}$
$i = 1$	1	$C\gamma_5$
$i = 2$	γ_5	C
$i = 3$	i	$C\gamma_4\gamma_5$

are important representatives (C denotes the charge conjugation operator in Dirac space). For such operators one usually fixes the source at an arbitrarily chosen lattice site (like the origin) and has to compute the quark propagator $(D + m)_{0x}^{-1}$ from this point to all other points on the lattice. This allows to compute the hadron propagator from this source to any other sink position. Averaging over the sink

operators in some timeslices then projects to vanishing sink 3-momentum. Summing over many gauge configurations amounts to averaging out all but the $\vec{p} = 0$ component of the correlator.

Next to such “local” operators, where all quarks live on the same lattice site, one can use extended operators combining quarks at different, nearby points (cf., [16] and references therein). This way one can utilize the lattice symmetries to construct representations of the cubic group. Such combinations correspond to certain combinations of angular momentum representation in the continuum. Such an approach involves the computation of more quark propagators, one for each sink position.

Another way to improve the signal is to use some type of smearing. One can locally average the gauge links (gauge configuration smearing). This should not affect the correlation function over larger time distance. One can, however, instead of point-like quark sources also use modified ones that are smeared over some region. In the BGR collaboration we used Gaussian smearing which refers to the Gaussian shape of the source [17, 2, 1]. Here one needs to compute quark propagators for each type of sink, e.g, for a narrow and a widely smeared sink. One then combines differently smeared quark propagators to hadron operators. This approach improves the statistical quality of the correlation functions significantly.

3.2 *The problem with excited states*

The real problem with excited states is that they are unstable, they decay. They are no asymptotic states of the theory and thus we cannot go to large time distances to identify them, we have to rely on other methods. Fortunately the finiteness of the lattice comes to the rescue. On a finite lattice the energy spectrum is not continuous but discrete. By studying the volume dependence of the spectrum one can learn about the scattering phase shift and other properties of the scattering amplitude. This has been studied in detail [18, 19, 20, 21] and first attempts to use this approach in full QCD simulations have been published [22, 23]. The central problem is to reliably determine the energy spectrum in lattice calculations.

In quenched simulations life is somewhat simpler: The states cannot decay since there is no creation of quark–anti-quark loops from the vacuum. The spectrum in some channel with definite quantum numbers is directly related to masses of excited states. There is, however, a shadow of dynamical quarks due to the quark-lines turning around and running backwards for some time (cf., the 2nd graph in Fig. 11). This may lead to effects mimicking intermediate 2-particle states. We come back to that problem, which leads to quenched ghosts, later on.

A correlation function between hadronic operators involves a sum over a tower of intermediate states, as can be seen inserting a complete set of (physical) mass eigenstates. Let us assume $X(t)$ denotes the operator with vanishing 3-momentum at Euclidean time t , then the correlator is

$$\langle X(t)\bar{X}(0) \rangle = \sum_n \langle X(t)|n \rangle e^{-m_n t} \langle n|\bar{X}(0) \rangle \quad (10)$$

$$\sim a_1 e^{-m_1 t} + a_2 e^{-m_2 t} + a_3 e^{-m_3 t} + \dots \quad (11)$$

The leading term with the smallest mass is the ground state, which will be dominantly seen at asymptotically large t . The other states are the excitations which we are interested in. They will be observed at smaller t and dominate the ground state signal. In the Monte Carlo calculation we have to somehow disentangle these states. Simply fitting to a sum of exponentials is usually unstable and needs extremely good statistics. Several better methods have been used.

The *Bayesian analysis* is based on ideas from Ref. [24] and has been used in extracting excited hadrons in a sequence of papers [25, 26]. This is a stepwise procedure, where one starts by extracting the ground state mass from larger t and then uses that value as a prior for getting estimates of the higher lying states at smaller t .

Another method combines correlation function values from different time slices such as to “subtract” the leading exponential behavior [27]; the combination leads to rapidly decaying correlators.

Another approach used was to reconstruct the spectral density (as a continuous function) with the *maximum entropy method* [28]. This method results in a probability function for the masses. One seems to need high (statistical) quality data for a successful application.

In the BGR collaboration [17, 2, 1] and also in the LHPC collaboration and the Adelaide group [29, 30, 16, 31] the so-called *variational method* is used. The idea is straightforward. In functional analysis a function can be expanded in a series of independent basis functions. In the same way the unknown operator of the physical state can be built from a sum over basis operators. Contrary to simple continuum mathematics, we do not know how to orthogonalize our interpolating field operators. We can, however, study correlation matrix elements between the set of interpolating operators,

$$C_{ij}(t) = \langle X_i(t) \bar{X}_j(0) \rangle . \quad (12)$$

Like in the spectral representation (10) these correlators will involve implicitly sums over the physical eigenstates. In [18, 20] it was shown, that the composition of the physical operators in terms of the interpolating operators can be recovered by solving the generalized eigenvalue problem,

$$C(t) u^{(n)} = \lambda^{(n)}(t) C(t_0) u^{(n)} . \quad (13)$$

The eigenvalues will, in leading order, behave like single exponentials and allow us to recover the energy (or for vanishing 3-momentum, the mass) values of the intermediate physical states:

$$\lambda^{(n)}(t) \approx e^{-E_n(t-t_0)} \left(1 + \mathcal{O} \left(e^{-\Delta E_n(t-t_0)} \right) \right) . \quad (14)$$

Here ΔE_n denotes the energy difference to the next higher state. The eigenvectors give an idea on the composition of the physical states and provide a fingerprint of the state.

There are some caveats. The number of possible interpolating fields is limited due to resources. Also, including too many of them adds statistical noise to the correlation matrix affecting the reliability of the diagonalization. Therefore it pays off to find “good” interpolators. One has to stress, however, that there is no a priori bias for the composition of the physical states, except for the choice of the basis set of interpolating fields.

Note that the diagonalization is done for each time distance t independently. Thus it is important to study the consistent identification of each state by following the eigenvectors. In practice one tries to find stability plateaus, such that the energy values and the eigenvectors remain constant over a range of t -values.

One can define effective masses

$$M_{\text{eff}} \left(t + \frac{1}{2} \right) = \ln(\lambda(t)/\lambda(t+1)) \quad (15)$$

for each eigenvalue $\lambda_n(t)$ and plot these like in Fig. 5 in order to get an idea on the plateau range. The fit to the final mass value is then done with an exponential fit over all points in the plateau range. The number of eigenvalues to be trusted is of course smaller than the order of the correlation matrix. It can be determined by studying the effect when enhancing or reducing the set of interpolators. The typical experience is that the lower 2/3 of the energy levels are reliable.

Combining different Dirac structures and differently smeared quark sources to hadron interpolators gives a large basis set [1, 2]. Not all of them bring in new content, though, and one tries to minimize their number in order to improve the statistical quality of the diagonalization result. Physical intuition guides the construction; a recent inclusion of derivative sources led to some improvement [32].

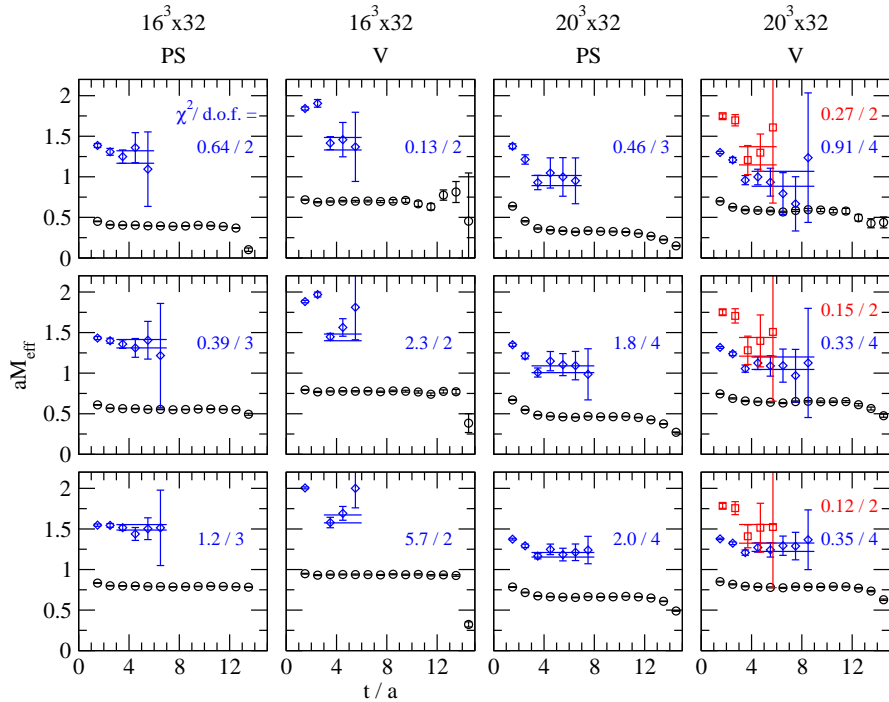


Figure 5: Effective-mass plots for pseudoscalar (PS) and vector (V) ground state mesons and first excitations for different size lattices (Fig. from [2]).

3.3 Further issues

Of course it would be interesting and important to study, e.g., the scalar isoscalar 0^{++} meson channel (f_0 , also called σ or ϵ depending on your favorite edition of the particle data booklet). This is rarely done so far. The reason is that the propagator for such a $\bar{u}u$ state involved disconnected, backtracking loops. In order to project to zero momentum one would need such loops for all L^3 sites of a timeslice, and thus compute L^3 quark propagators. Otherwise the signal would be extremely noisy. This is very costly and therefore one tries to invent methods (like low-mode averaging [33]) to improve the situation. Most groups avoid this problem by considering only hadron correlation functions which do not involve disconnected terms.

In principle 2-particle channels may obscure the single particle signal. Even in quenched calculations there may be quasi-2-particle states due to Z -shaped quark lines. A possible identification method is to study the volume dependence of the spectral weight [34]. For 2-particle states in the rest frame there may be relative spatial momenta, which then have a volume dependence via the spectral relation $E = 2\sqrt{m^2 + p^2}$, where p may be multiples of the minimum lattice momentum $2\pi/L$. Also studying the operators with non-vanishing total momentum allows one to distinguish single particle states from 2-particle states.

Finite volume quenches the states, leading to higher mass values for hadrons with large physical size. This and another effect related to light states (the pion) running around the usually periodic spatial lattice has to be considered as well.

As has been pointed out [35], in the quenched situation the Z -graph like contributions may mimic ghost states like an η' , leading to negative contributions to the propagator, in particular towards smaller quark masses. This has been verified in both, baryonic and mesonic channels [26, 34, 36]. The functional behavior of this contribution deviates from a simple exponential. The term has to be either removed with an ansatz for its shape [26, 34] or by isolating it in the variational method [36].

The approach towards smaller quark masses is cumbersome. In the quenched case there are addi-

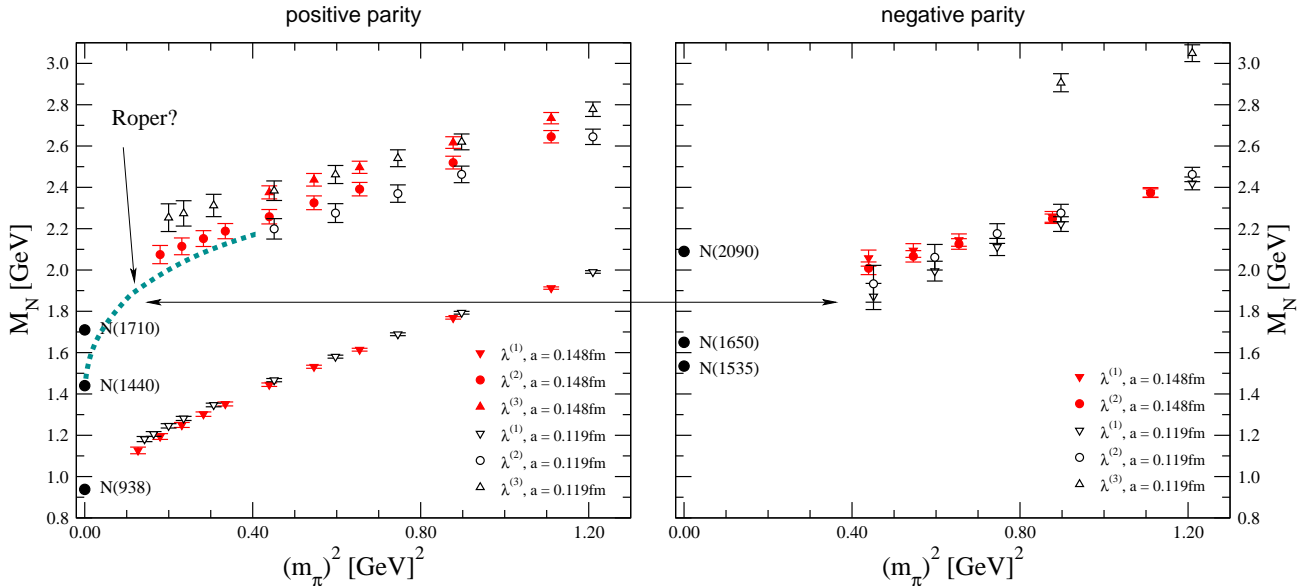


Figure 6: Quenched results for the positive and negative parity nucleons from Ref. [1]. The Roper states N(1440) and the N(1710) come out too high and there is no indication of level crossing.

tional singularities (quenched chiral logs). In the case with dynamical quark decay channel are opening and the identification of states like the ρ becomes more complicated.

4 Some results

4.1 Quenched results

In a quenched simulation [2, 1] we have generated gauge configurations with the Lüscher-Weisz gauge action [37] on lattices of size $16^3 \times 32$ and $20^3 \times 32$. The gauge coupling was chosen to work at lattice spacings between 0.12 and 0.15 fm, corresponding to a spatial lattice size around 2.4 fm. We used two mass-degenerate light quarks (u, d) and one heavier s-quark with its mass parameter adjusted to give the correct K-meson mass.

One of the open puzzles is the behavior of the first excitation in the positive parity nucleon channel, the so-called Roper resonance N(1440). In quantum mechanics and in the heavy quark limit the positive and negative parity excitations come with alternate parities (+ - + -). The experimentally observed states show a different order: N(940), N(1440), N(1535) and N(1650) corresponding to (+ + - -). Since in the lattice simulations we proceed from high to low quark masses we expect a level crossing at some point. So far, in the regions accessible to studies, only one group has seen such a crossing at smaller quark masses [26], albeit with large error bars. In that study smaller pion masses were accessible due to using the overlap action; the analysis was of the discussed Bayesian type. Other groups, including ours, identify the Roper state at high masses but its behavior is inconspicuous towards lower quark masses and no drastic change of slope is observed. Clearly there are two concerns: (a) the finite volume may quench the excited states enhancing their energy or (b) dynamical fermions may be important when approaching the chiral limit. No such deviation is noticed for the negative parity sector.

Chiral perturbation theory [6] (cf., the talks [38, 39]) is a systematic expansion around the chiral limit. The effective Lagrangian introduces parameters, which can be determined by comparing with experiment (or lattice results) [40, 41]. Expansion of the nucleon mass involves terms $\mathcal{O}(m)$, $\mathcal{O}(m^2) \propto m_\pi$, and so on, (the exact form depending on whether one uses quenched ChPT [42] or not). Excited

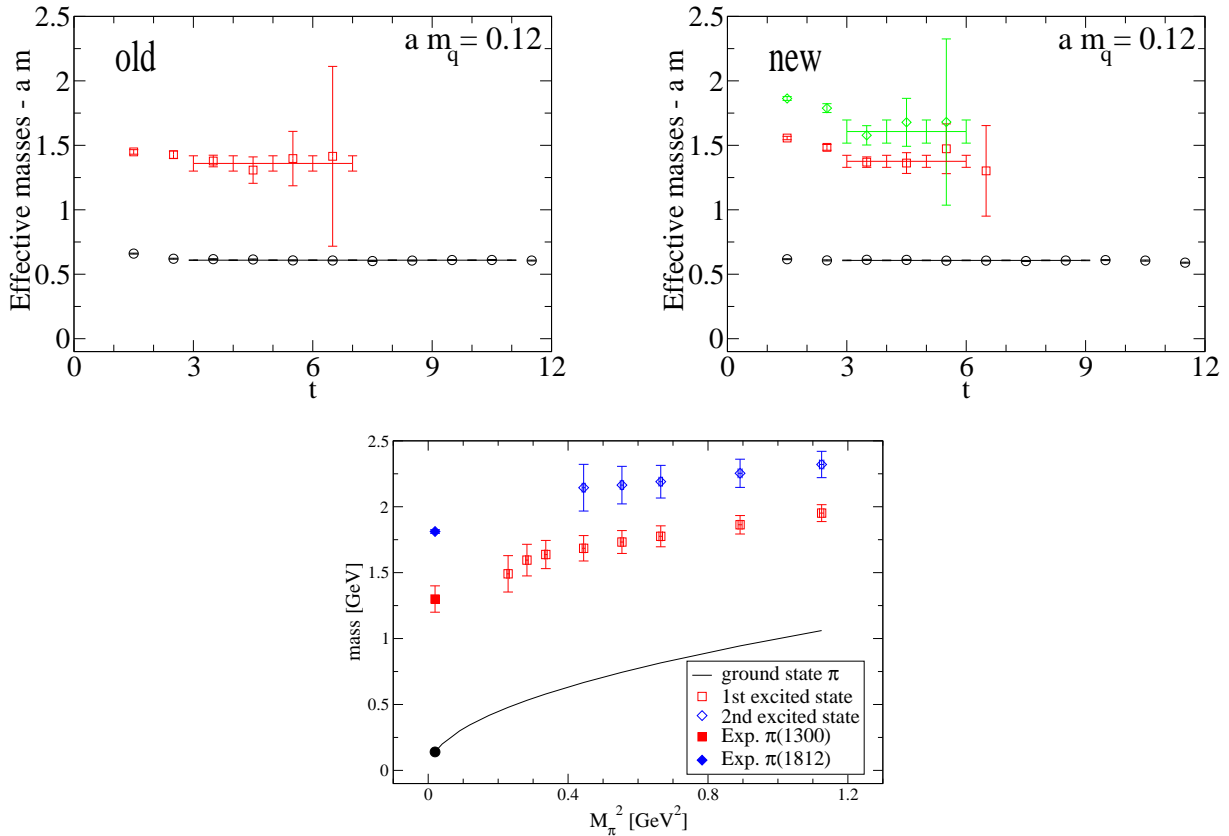


Figure 7: The upper two plots (from [32]) compare the results of an analysis of the pseudoscalar pion channel without (old) and with (new) derivative quark sources. The lower plot shows the obtained values for several valence quark masses. The ground state pion curve is plotted just to guide the eye.

states bring in new scales and new assumptions. In such an expansion around $M_\pi = 0$ the Roper and the ground state nucleon behave similarly [43].

Fig. 1 exhibits the results of a simple extrapolation to the physical point [1] and we have discussed some conclusions in the introduction. The agreement of the negative parity extrapolations is remarkable and led us to suggest to look for a negative parity state $\Omega(1970)$ and two Ξ states near 1780 MeV.

In the meson sector the discussed variational technique allowed us to clearly identify the first pseudoscalar and vector excitations. A recent extension of that study includes covariant (nearest neighbor) derivative quark sources, which introduce another set of interpolators. Indeed first results show that this allows one to obtain higher excitations in certain channels [32]. Fig. 7 demonstrates this improvement for the pseudoscalar channel.

4.2 Dynamical fermions

To include dynamical fermions in the Monte Carlo simulation means to include the determinant of the Dirac operator matrix as a weight factor in the generation of the gauge configurations. This is done by utilizing the relation between Grassmann and bosonic integration:

$$\det(D D^\dagger) = \int [\mathcal{D}\psi \mathcal{D}\bar{\psi}] \exp(-\bar{\psi}(D D^\dagger)\psi) = \int [\mathcal{D}\phi \mathcal{D}\phi^\dagger] \exp(-\phi^\dagger(D D^\dagger)^{-1}\phi). \quad (16)$$

The bosonic fields ϕ and ϕ^\dagger have the same degrees of freedom as the fermions and are called pseudo-fermions. In a simulation the change of the fermion determinant due to suggested changes of the gauge

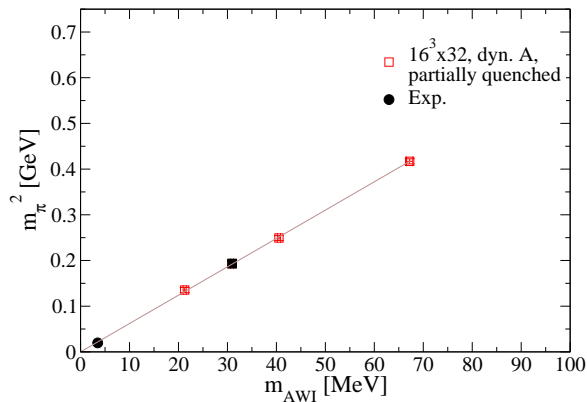


Figure 8: Pion mass squared vs. the quark mass for run A. The data point marked by the filled square (2nd from below) is the value where the valence quark and the sea quark masses agree, the other three points are partially quenched, i.e., the valence quark mass differs from the sea quark mass. In that plot the quark mass has been determined with help of the axial Ward identity (AWI) from the ratio of a correlators involving the derivative of the axial current and the pseudoscalar field, thus called m_{AWI} .

fields thus can be expressed through the bosonic variables. Due to the inversion of the matrix the effective bosonic action is very non-local and the simulation becomes expensive. The standard method is to evolve the gauge field in a molecular dynamics algorithm for some time and then correct for accumulated errors by a Monte-Carlo accept-reject step. This is called one trajectory in this so-called Hybrid Monte-Carlo (HMC) algorithm [44].

In the molecular dynamics part one has to compute the inverse and the derivative of the Dirac operators with regard to the changed gauge fields quite often. This is time consuming, in particular for more complicated actions with many terms like the CI action.

In [45] we have discussed our implementation of the HMC algorithm for the CI action and shown first results on $12^3 \times 16$ lattices. Meanwhile we have been extending the study to larger $16^3 \times 32$ lattices with a lattice spacing around 0.154 fm [46]. We use the Lüscher-Weisz gauge action, stout smearing and two mass-degenerate light quarks. The molecular dynamics trajectory has 100 steps for one unit of HMC-time and we analyze every 5th configuration to reduce autocorrelation. Up to the moment of the Erice meeting we have produce $\mathcal{O}(50)$ independent configurations for two combinations of mass and lattice spacing (cf., Table 1).

run	β_{LW}	c_0	n_{conf}	n_{meas}	a [fm]	M_π [MeV]
A	4.65	-0.06	425	65	0.153(1)	463(4)
B	4.70	-0.05	350	50	0.154(1)	507(5)

Table 1: Parameters of the two runs discussed: run sequence, gauge coupling, bare mass parameter c_0 , number of configurations n_{conf} , number of configurations analyzed n_{meas} , lattice spacing a assuming that the Sommer parameter is $r_0 = 0.48$ fm, pion mass.

In a simulation with dynamical quarks the sea quark mass agrees with the valence quark mass; thus one has just one data point, unlike a quenched simulation where one shows many different valence quark masses. In an attempt to better understand the difference one relies also in dynamical quark simulations on so-called partially quenched data points, where the valence quark mass differs from the sea quark mass. Fig. 8 shows such a result, where indeed the partially quenched values for the pion mass together with the only “correct” dynamical point (second square from the left) extrapolate nicely

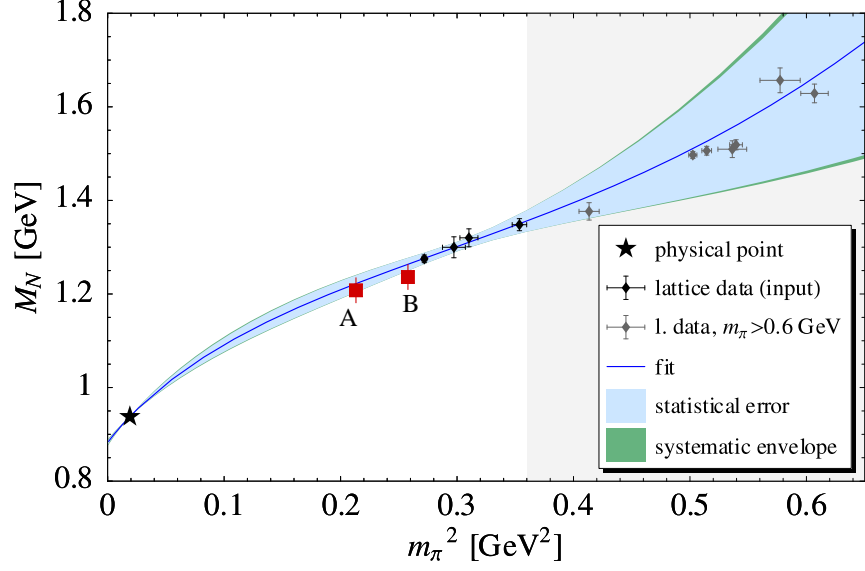


Figure 9: Our results for the CI-action HMC simulation (full squares) compared to the ChPT analysis error band and lattice data as discussed in Ref. [47] (original figure from that reference, data as quoted [48, 49]).

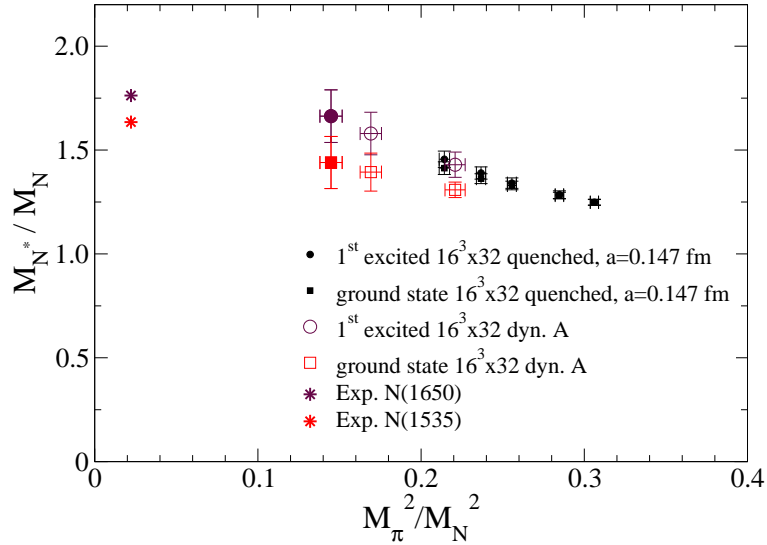


Figure 10: We can identify the two lowest lying negative parity nucleons [46] which are compatible with a smooth extrapolation to the experimental values.

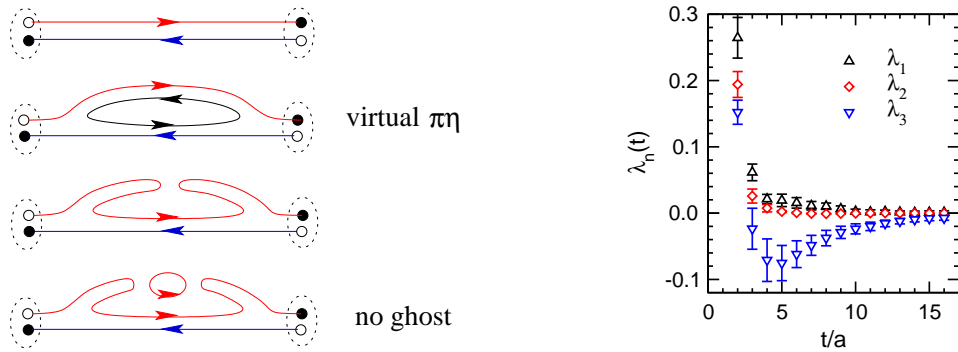


Figure 11: Left: Graphs contributing to the isovector channel; the 2nd and the 4th are missing in the quenched approximation. Right: One of the three leading eigenvalues in the quenched a_0 -correlation function shows the ghost contribution [36].

to the chiral limit. This is another example of the good agreement of lattice results with the (leading order ChPT) Gell-Mann–Oakes–Renner relation [50],

$$f_\pi^2 M_\pi^2 = -2 m \langle \bar{q}q \rangle . \quad (17)$$

Comparing our results for the nucleon mass with, e.g., the chiral analysis of Ref. [47], we find (see Fig 9) excellent agreement with the chiral interpolation between the experimental nucleon mass and other lattice results.

Our results for dynamical quarks brought no surprises for the negative parity nucleons (Fig. 10). We continue to find two nearby states extrapolating to the physical value towards the smaller quark masses, behavior and values very similar to the quenched situation.

A particularly problematic mesonic channel is that of the isovector, scalar meson a_0 . In quenched calculations this channel is plagued by an artifact. In Fig. 11 the quark lines contributing to the propagator are indicated. In the quenched case only the 1st and 3rd diagrams contribute. As discussed earlier, the 3rd diagram gives, for small quark masses, rise to a virtual $\pi\eta'$ ghost state, which adds a negative contribution to the total propagator [35, 26, 34]. The right-hand side plot (from Ref. [36]) shows such a contribution; it decouples in the variational approach, but due to limited statistics this decoupling is not perfect at smaller masses, rendering the extrapolation of the a_0 -mass towards smaller quark masses problematic.

In quenched calculations the a_0 -mass was always seen too high, compatible with the first excitation $a_0(1450)$. The behavior in the dynamical runs came as a surprise. We now see the lowest mass compatible with the ground state $a_0(980)$ (see Fig. 12).

In full QCD the 4th diagram in Fig. 11 removes the ghost behavior, the $\pi\eta$ channel now couples as a physical state. Also, since we have relatively high quark masses $\mathcal{O}(30 \dots 40)$ MeV, the now possible quark vacuum loops cannot really distinguish between light and heavy (strange) quark contributions. Since this 2-particle channel mixes with the a_0 state we will have to study its momentum, volume and quark mass dependence to make sure that the observed energy value corresponds really to a single particle mass [51].

5 Summary and conclusion

Although lattice calculations have gone a long way, there are still hard challenges ahead. Excited studies for full QCD requires systematic exploration of volume dependence, quark mass dependence and scaling towards the continuum limit. First steps in determining properties of excited states (like

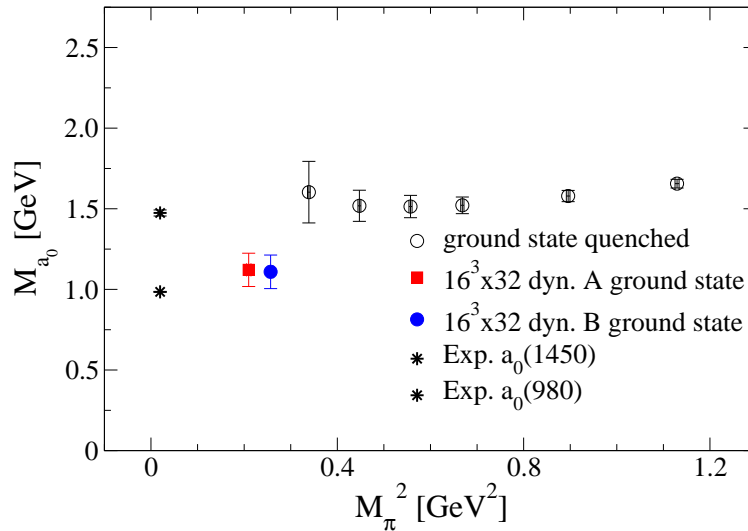


Figure 12: Whereas in the quenched case we (like other authors) obtain a a_0 -mass which points towards the $a_0(1450)$, the dynamical results seem to indicate a low lying state compatible with $a_0(980)$.

decay constants) are under progress [52]. The puzzle of the Roper state and its level crossing should be clarified. The future is wide open.

6 Acknowledgment

I want to thank the organizers for the enjoyable meeting. Special thanks go to all my collaborators in the BGR collaboration for many years of challenging and fruitful cooperation, in particular to T. Burch, R. Frigori, C. Gattringer, L.Y. Glozman, C. Hagen, P. Hasenfratz, D. Hierl, Ph. Huber, M. Limmer, P. Majumdar, T. Maurer, D. Mohler, F. Niedermayer, W. Ortner, and A. Schäfer.

References

- [1] T. Burch et al., *Phys. Rev. D* 74 (2006) 014504, hep-lat/0604019.
- [2] T. Burch et al., *Phys. Rev. D* 73 (2006) 094505, hep-lat/0601026.
- [3] L.Y. Glozman, *Phys. Rept.* 444 (2007) 1, hep-ph/0701081.
- [4] K.G. Wilson, *Phys. Rev. D* 10 (1974) 2445.
- [5] M. Creutz, *Phys. Rev. D* 21 (1980) 2308.
- [6] S. Weinberg, *Physica A* 96 (1979) 327. J. Gasser and H. Leutwyler, *Ann. Phys.* 158 (1984) 142.
- [7] H.B. Nielsen and M. Ninomiya, *Phys. Lett. B* 105 (1981) 219; *Nucl. Phys. B* 185 (1981) 20; *Nucl. Phys. B* 193 (1981) 173.
- [8] P.H. Ginsparg and K.G. Wilson, *Phys. Rev. D* 25 (1982) 2649.
- [9] P. Hasenfratz and F. Niedermayer, *Nucl. Phys. B* 414 (1994) 785. A. Hasenfratz, P. Hasenfratz and F. Niedermayer, *Phys. Rev. D* 72 (2005) 114508, hep-lat/0506024.
- [10] H. Neuberger, *Phys. Lett. B* 417 (1998) 141; *ibid.* B 427 (1998) 353.
- [11] M. Lüscher, *Phys. Lett. B* 428 (1998) 342.
- [12] D.B. Kaplan, *Phys. Lett. B* 288 (1992) 342, hep-lat/9206013.
- [13] V. Furman and Y. Shamir, *Nucl. Phys. B* 439 (1995) 54, hep-lat/9405004.

- [14] C. Gattringer, *Phys. Rev. D* 63 (2001) 114501, hep-lat/0003005. C. Gattringer, I. Hip and C.B. Lang, *Nucl. Phys. B* 597 (2001) 451, hep-lat/0007042.
- [15] C. Gattringer et al. (BGR (Bern-Graz-Regensburg) collaboration), *Nucl. Phys. B* 677 (2004) 3, hep-lat/0307013.
- [16] R.G. Edwards et al. (LHPC collaboration), *PoS LATTICE2007* (2007) 108, arXiv:0710.3571 [hep-lat].
- [17] T. Burch et al., *Phys. Rev. D* 70 (2004) 054502, hep-lat/0405006. T. Burch et al., *PoS LAT2005* (2005) 097, hep-lat/0509086.
- [18] C. Michael, *Nucl. Phys. B* 259 (1985) 58.
- [19] M. Lüscher, *Commun. Math. Phys.* 105 (1986) 153.
- [20] M. Lüscher and U. Wolff, *Nucl. Phys. B* 339 (1990) 222.
- [21] M. Lüscher, *Nucl. Phys. B* 354 (1991) 531; *ibid.* B 364 (1991) 237.
- [22] C. McNeile and C. Michael, *Phys. Lett. B* 556 (2006) 177, hep-lat/0212020.
- [23] S. Aoki et al., *PoS LAT2006* (2006) 110, hep-lat/0610020. S. Aoki et al., *Phys. Rev. D* 76 (2007) 094506, arXiv:0708.3705v1.
- [24] G.P. Lepage et al., *Nucl. Phys. Proc. Suppl.* 106 (2002) 12, hep-lat/0110175.
- [25] F. Lee et al., *Nucl. Phys. Proc. Suppl.* 119 (2003) 296, hep-lat/0208070. Y. Chen et al., The Sequential Empirical Bayes Method: An Adaptive Constrained-Curve Fitting Algorithm for Lattice QCD, hep-lat/0405001.
- [26] S.J. Dong et al., *Phys. Lett. B* 605 (2005) 137, hep-ph/0306199.
- [27] D. Guadagnoli, M. Papinutto and S. Simula, *Phys. Lett. B* 604 (2004) 74, hep-lat/0409011 .
- [28] K. Sasaki, S. Sasaki and T. Hatsuda, *Phys. Lett. B* 623 (2005) 208, hep-lat/0504020.
- [29] W. Melnitchouk et al., *Phys. Rev. D* 67 (2003) 114506, arXiv:hep-lat/0202022v3. J. M. Zanotti et al., *Phys. Rev. D* 68 (2003) 054506, hep-lat/0304001.
- [30] B.G. Lasscock et al., *Phys. Rev. D* 76 (2007) 054510, arXiv:0705.0861
- [31] S. Basak et al., *Phys. Rev. D* 72 (2005) 094506, hep-lat/0506029; *ibid.* *Phys. Rev. D* 72 (2005) 074501 hep-lat/0508018, . *Nucl. Phys. (Proc. Suppl.)* 153 (2006) 242, hep-lat/0601034. *PoS LAT2006* (2006) 197, hep-lat/0609072. *Phys. Rev. D* 76 (2007) 074504, arXiv:0709.0008.
- [32] C. Gattringer et al., *PoS LATTICE 2007* (2007) 123, arXiv:0709.4456.
- [33] T. DeGrand and S. Schaefer, *Nucl. Phys. Proc. Suppl.* 140 (2005) 296, hep-lat/0409056; *Comput. Phys. Commun.* 159 (2004) 185, hep-lat/0401011
- [34] N. Mathur et al., Scalar Mesons $a_0(1450)$ and $\sigma(600)$ from Lattice QCD, hep-ph/0607110.
- [35] W.A. Bardeen et al., *Phys. Rev. D* 65 (2001) 014509, hep-lat/0106008.
- [36] T. Burch et al., *Phys. Rev. D* 73 (2006) 017502, hep-lat/0511054.
- [37] M. Lüscher and P. Weisz, *Commun. Math. Phys.* 97 (1985) 59; *ibid.* 98 (1985) 433.
- [38] A. Thomas, Hadron structure and quark models - the “spin crisis”, Contribution to these proceedings, 2007.
- [39] W. Weise, Chiral extrapolations of nucleon properties, Contribution to these proceedings, 2007.
- [40] U.G. Meissner, *PoS LAT2005* (2006) 009, hep-lat/0509029.
- [41] J. Bijnens, *PoS LATTICE2007* (2007) 004, arXiv:0708.1377 [hep-lat]
- [42] J.N. Labrenz and S.R. Sharpe, *Phys. Rev. D* 54 (1996) 4595, hep-lat/9605034.
- [43] B. Borasoy et al., *Phys. Lett. B* 641 (2006) 294, hep-lat/0608001.
- [44] S. Duane et al., *Phys. Lett. B* 195 (1987) 216.

- [45] C.B. Lang, P. Majumdar and W. Ortner, *Phys. Rev. D* 73 (2006) 034507, hep-lat/0512014.
- [46] R. Frigori et al., *PoS LATTICE2007* (2007) 114, arXiv:0709.4582v1 [hep-lat].
- [47] M. Procura et al., *Phys. Rev. D* 73 (2006) 114510, hep-lat/0603001.
- [48] A. Ali Khan et al., *Nucl. Phys. B* 689 (2004) 175, hep-lat/0312030.
- [49] B. Orth, T. Lippert and K. Schilling, *Phys. Rev. D* 72 (2005) 014503, hep-lat/0503016.
- [50] M. Gell-Mann, R.J. Oakes and B. Renner, *Phys. Rev.* 175 (1968) 2195.
- [51] C. McNeile and C. Michael, *Phys. Rev. D* 74 (2006) 014508, arXiv:hep-lat/0604009. C. McNeile, *PoS LATTICE2007* (2007) 019, arXiv:0710.0985.
- [52] C. McNeile and C. Michael, *Phys. Lett. B* 642 (2006) 244, hep-lat/0607032. C. McNeile, Lattice Approach to Light Scalars, arXiv:0710.2470 [hep-lat]